Cellular Uptake and Intracellular Localization of Benzo(a)pyrene by Digital Fluorescence Imaging Microscopy

ANNE L. PLANT, DOUGLAS M. BENSON, and LOUIS C. SMITH
Departments of Medicine, Biochemistry, and Cell Biology, Baylor College of Medicine and The Methodist Hospital, Houston, Texas 77030

ABSTRACT Uptake of benzo(a)pyrene by living cultured cells has been visualized in real time using digital fluorescence-imaging microscopy. Benzo(a)pyrene was noncovalently associated with lipoproteins, as a physiologic mode of presentation of the carcinogen to cells. When incubated with either human fibroblasts or murine P388D_1 macrophages, benzo(a)pyrene uptake occurred in the absence of endocytosis, with a halftime of ~2 min, irrespective of the identity of the delivery vehicles, which were high density lipoproteins, low density lipoproteins, very low density lipoproteins, and 1-palmitoyl-2-oleoylphosphatidylcholine single-walled vesicles. Thus, cellular uptake of benzo(a)pyrene from these hydrophobic donors occurs by spontaneous transfer through the aqueous phase. Moreover, the rate constant for uptake, the extent of uptake, and the intracellular localization of benzo(a)pyrene were identical for both living and fixed cells. Similar rate constants for benzo(a)pyrene efflux from cells to extracellular lipoproteins suggests the involvement of the plasma membrane in the rate-limiting step. The intracellular location of benzo(a)pyrene at equilibrium was coincident with a fluorescent cholesterol analog, *N*-(7-nitrobenz-2-oxa-1,3-diazole)-23,24-*dinor*-5-cholen-22-amine-3β-ol. Benzo(a)pyrene did not accumulate in acidic compartments, based on acridine orange fluorescence, or in mitochondria, based on rhodamine-123 fluorescence. When the intracellular lipid volume of isolated mouse peritoneal macrophages was increased by prior incubation of these cells with either acetylated low density lipoproteins or with very low density lipoproteins from a hypertriglyceridemic individual, cellular accumulation of benzo(a)pyrene increased proportionately with increased [1-^{14}C]oleate incorporation into cellular triglycerides and cholesteryl esters. Thus, benzo(a)pyrene uptake by cells is a simple partitioning phenomenon, controlled by the relative lipid volumes of extracellular donor lipoproteins and of cells, and does not involve lipoprotein endocytosis as an obligatory step.

Benzo(a)pyrene is a common environmental pollutant whose carcinogenic potential depends on oxidative metabolism after cellular uptake (1). Oxygenation and hydration reactions occur in the endoplasmic reticulum to form active carcinogenic compounds, such as diol expoxides, that interact covalently with DNA. Most investigations have been concerned with the enzymatic events of cytochrome P_{450}-dependent metabolic processes, and with the chemical modification of DNA. In vivo, these processes are necessarily preceded by cellular uptake of the hydrophobic precursor hydrocarbon (2). Typically, metabolic studies of benzo(a)pyrene are performed by exposing cells or microsomal fractions to concentrated solutions of benzo(a)pyrene in organic solvents diluted into the culture medium or the reaction mixture. Because of the low aqueous solubility of benzo(a)pyrene, ~10^{-8} M (3), little of the hydrocarbon is truly in solution under these conditions and most, if not all, is present in the form of microcrystals (4). The kinetics of desorption of benzo(a)pyrene from microcrystals to lipid bilayers is slow (5). Because solubilization of benzo(a)pyrene in microsomal membranes is obligatory for its further metabolism, this experimental procedure most likely leads to significant underestimation of the rate and extent of metabolism, because there is limited incorporation of benzo(a)pyrene into microsomal preparations or cell membranes.

A physiologic mode of presentation of these hydrophobic compounds is as a solubilized component of a lipid matrix. Studies in vitro (6, 7) and in vivo (8) have shown that

THE JOURNAL OF CELL BIOLOGY · VOLUME 100 APRIL 1985 1295-1308

benzo(a)pyrene and dimethylbenzanthracene, respectively, are present in the plasma as noncovalent components of the plasma lipoproteins. The plasma lipoproteins are dynamic macromolecular assemblies of lipids and specific apoproteins and differ in size, density, chemical composition, and metabolic fate (9, 10). In fasting plasma, the most abundant lipoproteins are the protein-rich high density lipoproteins (HDL),[1] which contain about 25 mol% phosphatidylcholine and 50 mol% protein. Low density lipoproteins (LDL) contain 37 mol% cholesteryl ester, whereas very low density lipoproteins (VLDL) are 50 mol% triglyceride. Apolipoprotein B (ApoB) a protein component of LDL, is recognized by specific high-affinity membrane sites on certain cells for receptor-mediated endocytosis (11). Thus, uptake of LDL by these receptors could introduce benzo(a)pyrene and other xenobiotics into the cell interior as components of the lipoprotein.

The lipids and most of the protein components of lipoproteins exchange rapidly among lipoprotein classes (9, 10). Benzo(a)pyrene transfer between LDL is relatively fast, with a halftime of ~200 ms (12). Many factors are known to influence the rates and energetics of spontaneous desorption of lipophiles such as fatty acids, phospholipids, and polycyclic aromatic hydrocarbons from a phospholipid surface. These include the length of acyl chains (13), the nature of the hydrophilic headgroup (13–15), the molecular surface area of aromatic compounds (16), the nature of the hydrophobic environment (17, 18), and the radius of the lipid surface from which desorption occurs (19).

Evidence that cellular uptake of benzo(a)pyrene from lipoproteins occurs by transfer of individual molecules through the aqueous solution has been obtained by Remsen and Shireman (20), who have demonstrated with LDL receptor-negative cells that cellular uptake of benzo(a)pyrene can occur in the absence of LDL endocytosis. These studies, however, did not address the kinetics of passive transfer of benzo(a)pyrene, or the potential contribution in normal cells of either receptor-mediated endocytosis or fluid-phase endocytosis of the lipoprotein carrier. Clarification of these aspects of the dynamics of cellular uptake of benzo(a)pyrene and the mechanism of intracellular and intercellular distribution of benzo(a)pyrene is necessary to understand the overall process of benzo(a)pyrene carcinogenesis. Thus, one objective of this study was to examine the mechanism and kinetics of benzo(a)pyrene entry into cells by direct observation of living cells in real time using digital fluorescence-imaging microscopy. A second objective was to determine the effects of lipoprotein metabolism on the extent of cell uptake and on intracellular distribution of benzo(a)pyrene. An abstract of this work has been published (21).

MATERIALS AND METHODS

Fluorescence Microscopy: The digital fluorescence-imaging microscopy system is described in detail in the preceding article (22). Briefly, the system consisted of a Leitz Diavert inverted fluorescence microscope (E. Leitz, Inc., Rockleigh, NJ), a Hamamatsu Vidicon C1000-12 low light level camera (Hamamatsu Corp., Middlesex, NJ), and a Grinnell 274 image processor (Grinnell Systems Corp., San Jose, CA) with three separate 512 × 480 8-bit memory planes. A Lab Datex LSI 11/23 minicomputer (Data Translation, Inc., Marlboro, MA) was interfaced through a Q-bus to the image processor, a Charles River (Charles River Data Systems, Inc., Framingham, MA) 20 Mbyte hard disk and a Cipher F880 magnetic tape (Cipher Data Products Inc., San Diego, CA) for archival storage. Photographs of the Grinnell images were produced with a Matrix Instruments 35-mm color graphic recorder (Matrix, Inc., Mesa, AZ).

Cells were cultured as described below on 22-cm^2 × 0.17-mm glass coverslips in tissue culture dishes, and were transferred to Bionique culture chambers (Bionique, Corning, Lake Placid, NY) for experiments on the microscope. Live cells were maintained on the microscope stage at constant temperature (37° ± 1°C) with constant infusion of 5% CO_2. Cellular fluorescence was measured for 1 s at intervals of 30 s or 1 min. Typical fields contained one to three fibroblasts and 12–20 macrophages. Single frames were digitized in 33 ms. To increase the signal-to-noise ratio, each image that was stored was an integration of 32 frames acquired at 30 Hz. To avoid photofading, excitation light was reduced with neutral-density filters. The absence of photofading was verified by rate constant maps (22). In the microscope field of 111 × 128 μm, pixel size was ~0.0625 μm^2 at the magnification used for this study. Time lapse video recording of the phase-contrast images allowed evaluation of viability of cells by the saltatory movement of the phase-dense lysosomes (23).

Lipoprotein Preparation: Lipoproteins were isolated from normal human plasma by ultracentrifugation (24) at the following densities: normal VLDL, $\rho < 1.006$; LDL, ρ 1.019–1.063; HDL, ρ 1.063–1.21. Lipoprotein-deficient serum was prepared from the fraction with $\rho > 1.21$. Hypertriglyceridemic VLDL (htg VLDL) with an S_f of 100–400 was prepared from plasma of a type IV individual by flotation (25). Acetylated LDL (acLDL) was prepared as described by Basu et al. (26). Lipoproteins were labeled with benzo(a)pyrene, [G-^{3}H]benzo(a)pyrene, or *N*-(7-nitrobenz-2-oxa-1,3-diazole)-23,24-*dinor*-5-cholen-22-amine-3β-ol (NBD-cholesterol) (27) by drying organic solutions of the fluorophore on 200-μm glass beads (Polysciences, Inc., Warrington, PA), and incubating the lipoprotein preparation with the beads overnight at 37°C. Approximately 0.2 μmol of benzo(a)pyrene was incorporated per milligram of LDL protein, which is equivalent to an average of 100 benzo(a)pyrene molecules per LDL. Benzo(a)pyrene content of labeled of HDL and VLDL was 0.017 and 0.1 $\mu mol \cdot mg^{-1}$ apoprotein, or an average of 1.7 and 60 benzo(a)pyrene molecules per lipoprotein, respectively. Benzo(a)pyrene labeling was quantified by optical density measurements on a Cary 15 spectrophotometer using an extinction coefficient of $6 \times 10^4\ M^{-1} \cdot cm^{-1}$ at 365 nm (28). LDL and HDL were labeled with 1,1′-dioctadecyl-3,3,3′,3′-tetramethylindocarbocyanine (dil) as described (29). Lipoproteins labeled with both dil and benzo(a)pyrene were labeled initially with dil, and then were labeled with benzo(a)pyrene.

Cell Culture: All cells were maintained at 37°C and 5% CO_2. Normal human fibroblasts were prepared from human foreskin explants and cultured in Dulbecco's modified Eagle's medium containing 10% fetal calf serum, 1 mM glutamine, and 50 $\mu g \cdot ml^{-1}$ penicillin/streptomycin. To induce LDL receptor expression, fetal calf serum was replaced with human lipoprotein-deficient serum for 2 days (11). C3H/10T ½ murine fibroblasts were obtained from the American Type Culture Collection and cultured in Dulbecco's medium supplemented with 10% fetal calf serum, 1 mM glutamine, and 50 $\mu g \cdot ml^{-1}$ penicillin/streptomycin. Cells were passaged before reaching confluence and were used between the 7th and the 11th passage. The P388D_1 murine macrophage cell line was obtained from the Salk Institute Cell Repository and was cultured in RPMI-1640 medium supplemented with 10% fetal calf serum, 1 mM glutamine, and 50 $\mu g \cdot ml^{-1}$ penicillin/streptomycin. Mouse peritoneal macrophages were isolated from Balb/c mice by peritoneal lavage. Isolated macrophages were cultured for 2 d under the conditions used for the continuous macrophage line.

Fluorescence Labeling of Cells: Benzo(a)pyrene was purchased from Aldrich Chemicals (Milwaukee, WI) and purified by thin-layer chromatography on silica gel in isooctane/ether/acetic acid (75:25:2, vol/vol/vol), or by reversed phase octadecyl-silica high-pressure liquid chromatography in 80% acetonitrile. DiI and rhodamine-123 were obtained from Molecular Probes (Junction City, OR), and acridine orange was purchased from Polysciences, Inc. The synthesis of NBD-cholesterol has been described (27). Live fibroblasts previously incubated with benzo(a)pyrene were exposed to 5 $\mu g \cdot ml^{-1}$ rhodamine-123 for 30 min at 37°C. Cells were placed in fresh medium for 10 min, transferred to the stage of the microscope, and viewed immediately. Rhodamine fluorescence was observed using a 560-nm band-pass filter for excitation and a 575-nm cut-on filter for emission. Acridine orange was added to live cells on the stage at a final concentration of 5 $\mu g \cdot ml^{-1}$. After 2 min, cells were rinsed twice with fresh medium and fixed. Acridine orange fluorescence was viewed immediately with a 480-nm bandpass plus a 495-nm cutoff filter for excitation and a 510-nm cut-on emission filter. Because of organelle movement in live

[1] *Abbreviations used in this paper:* acLDL, acetylated low density lipoprotein; DiI, 1,1′-dioctadecyl-3,3,3′,3′-tetramethylindocarbocyanine; HDL, high density lipoproteins; htg; hypertriglyceridemic; LDL, low density lipoproteins; NBD-cholesterol, *N*-(7-nitrobenz-2-oxa-1,3-diazole)-23,24-*dinor*-5-cholen-22-amine-3β-ol; VLDL, very low density lipoprotein.

cells, fixation of cells after labeling with acridine orange was required for colocalization studies. Gross cellular morphology was unchanged as a result of fixation, and the intracellular location of acridine orange, but not rhodamine-123, was identical before and for ~20 min after fixation.

NBD-cholesterol was added to fixed cells as a component of LDL for 12–24 h before viewing. For double-label experiments, cell were exposed to benzo(a)pyrene after labeling with NBD-cholesterol. NBD-cholesterol fluorescence was visualized through the same filter combination as acridine orange. For all double-label experiments, control cells labeled with one of each fluorophore were examined to quantify the appearance of fluorescence through the filter combination used for the other fluorophore. Control cells without any label were also examined for autofluorescence. Neutral-density filters were used to attenuate excitation light so that contributions from autofluorescence and/or fluorescence from the second fluorophore were below the limits of detection. Thus, the fluorescence intensity in any of the filter combinations was from emission of a single fluorophore. To establish limits of detection and the range of linear camera response, 1 ml of ethanolic solutions of benzo(a)pyrene, ranging from 0.1 to 200 μM, was added to the culture chamber. Excitation light was attenuated to 1% of maximum intensity for all samples except for the 150 and 200 μM samples, for which excitation light was attenuated to 0.4%. Fluorescence intensities of ethanolic solutions of dil, NBD-cholesterol, acridine orange, and rhodamine-123 concentrations were linear between 0.1 μM–1 mM, 0.1–80 μM; 0.1–50 μM; 0.1–100 μM, respectively. Excitation light was attenuated from 0 to 96.6%. The system response was a linear function of concentrations over this range.

The relation between fluorescence emission and intensity of excitation light is $I_f = I_o \times \phi(1 - e^{-\epsilon cl})$, where I_f is the fluorescence intensity; I_o, the intensity of excitation light; ϕ, quantum efficiency; ϵ, molar extinction coefficient; c, concentration; and l, pathlength of the sample. Because the pathlength of a lipid inclusion is small, <10 μm, the exponential term is small even at concentrations >500 μM. When the fraction of light absorbed is very small, such that ϵcl is <0.05, the fluorescence intensity is linear with concentration (30) and with mass (31). Even at concentrations >120 μM, fluorescence intensity in this system is proportional to mass, because of the front surface emission. Based on comparison of intensities of the standard solutions with intracellular fluorescence intensities, typical intracellular benzo(a)pyrene concentrations measured by digital fluorescence microscopy range appear to be within the linear range of the system response.

Benzo(a)pyrene Metabolism: Normal human fibroblasts and C3H10/T ½ murine fibroblasts were grown in parallel in 60-mm culture dishes until nearly confluent. At appropriate times, 1 ml of Dulbecco's medium containing 50 $\mu g \cdot ml^{-1}$ LDL labeled with [G-^{3}H]benzo(a)pyrene was added per plate. Final concentration of benzo(a)pyrene per dish was 10 μM. All plates were harvested simultaneously. Media were removed, combined with 1 ml of a 0.15 M NaCl rinse into tubes wrapped with aluminum foil, and lyophilized overnight. Cells were removed from dishes by scraping with a rubber policeman. Aliquots of cell suspensions were taken for protein determination (32), for scintillation counting, for calculation of recovery, and for extraction. A 0.5-ml volume of cell suspension was extracted twice with 5 ml of ethyl acetate/acetone (2:1, vol/vol). Extracts were dried under a N_2 stream, resolubilized, and applied to silica gel chromatogram sheets (Eastman Kodak Co., Rochester, NY) for separation of benzo(a)pyrene and metabolites. The solvent was hexane/benzene (15:1, vol/vol) (33). In this system, benzo(a)pyrene migrates near the solvent front, while metabolites remain near the origin. The benzo(a)pyrene band was identified by fluorescence. Each strip was then cut into sections and counted. Radioactivity left in the cell residue after extraction was assumed to be covalently bound metabolites. Media samples were extracted, chromatographed, and counted. Recovery of initial radioactivity was ~90%.

[^{14}C]Oleate/[^{3}H]Benzo(a)pyrene Incorporation: Macrophages were isolated from Balb/c mice by peritoneal lavage. After incubation for 2 d with either 50 $\mu g \cdot ml^{-1}$ LDL, acLDL, or htg VLDL in Dulbecco's medium containing 10% lipoprotein-deficient serum and 0.15 mM [1-^{14}C]-oleate (sp act, 1.2×10^7 cpm $\cdot \mu mol^{-1}$) complexed with bovine serum albumin (bovine serum albumin) (34) was added to each plate. After 38 h at 37°C, media were removed and cells were washed two times with 0.04 M Tris, pH 7.4, containing 0.15 M NaCl and 5 $mg \cdot ml^{-1}$ bovine serum albumin. Each plate was then incubated for 1 h in medium containing 10% lipoprotein-deficient serum and 100 $\mu g \cdot ml^{-1}$ LDL containing [G-^{3}H]benzo(a)pyrene (sp act 1.3×10^8 cpm $\cdot \mu mol^{-1}$). Cells were rinsed two times and then scraped into 1 ml of 0.15 M NaCl. Aliquots were taken for ^{3}H and protein quantification and for extraction of triglycerides and cholesteryl esters with 10 vols of hexane/2-propanol (3:2, vol/vol). Extracts were taken to dryness, redissolved in hexane, and chromatographed on Eastman silica gel chromatogram sheets in 2,2,4-trimethylpentane/ether/acetic acid (85:15:2, vol/vol/vol). Lipids were visualized with I_2 vapor, and the appropriate bands were cut out and counted. Macrophages on coverslips treated in parallel were fixed with 2% formaldehyde after treatment with benzo(a)pyrene.

Kinetic Measurements and Analysis: Kinetic measurements, based on time-dependent changes in cellular fluorescence intensity, were made directly. Fibroblasts were grown on 22-cm^2 No. 1 glass coverslips (Chase Instruments Corp., Poultney, VT), and placed in a teflon culture chamber designed for microscopy (Bionique, Corning, Lake Placid, NY). A plexiglass cover fitted with a stainless steel 15-gauge needle allowed perfusion with humidified 5% CO_2. Temperature control was achieved by hot air curtains. Ports in the chamber cover allowed constant monitoring of temperature, as well as removal and addition of media to cells on the stage. For kinetic experiments, the fluorescence of a single field of live or fixed cells was followed directly, in real time, after the addition of benzo(a)pyrene-labeled LDL in medium to the chamber to initiate cellular uptake. The field was monitored continually by phase contrast and exposed to excitation light at selected intervals. At each time point, phase and fluorescence images were digitized and stored.

Background fluorescence from the medium was not >5% greater than dark current values. Because of the large numerical aperture (1.4) and short depth of field (0.4 μm) of the ×63 objective lens, cellular fluorescence was minimally affected by fluorescence from labeled lipoproteins in the medium. These conditions allowed rapid, real-time measurements of the spatial distribution of cellular fluorescence. Therefore, cellular fluorescence measurements were not corrected for any contribution from the medium.

To quantify cellular uptake of [G-^{3}H]benzo(a)pyrene from lipoproteins, cells were separated from labeled lipoproteins by filtration through glass fiber filters. Filter assays were performed with fibroblasts suspended by trypsinization or with P388D$_1$ cells suspended by rinsing the plate with medium. Cells were suspended in 1.5–2 ml of either 0.15 M saline or culture medium without serum. Cell suspensions were stirred constantly with small magnetic bars. Temperature was measured with a Bailey digital thermometer (Bailey Instruments Co., Inc., Saddle Brook, MA). Small volumes of [G-^{3}H]benzo(a)pyrene-labeled lipoproteins were added to cell suspensions. At appropriate intervals, 50- or 100-μl aliquots were removed, added to 5 ml of buffer solution containing 0.15 M NaCl, 0.04 M Tris, 0.3 mM EDTA, and 5 $mg \cdot ml^{-1}$ bovine serum albumin, and filtered. Bovine serum albumin reduced nonspecific binding of benzo(a)pyrene-labeled LDL to the filters. For each experiment, a solution containing only [G-^{3}H]benzo(a)pyrene LDL was filtered to determine the background binding. In the absence of cells, filters bound between 2 and 5% of total counts. Filters were counted in scintillation fluid without further processing. Determination of cellular protein bound to filters indicated that the numbers of cells trapped were highly reproducible. As the uptake approached equilibrium, the relative differences in amounts of benzo(a)pyrene entering cells were small. To establish that differences in cellular [^{3}H]benzo(a)pyrene at the later time points were significantly above background levels, aliquots of the reaction mixture were counted without filtering and compared with the cellular radioactivity at equilibrium.

Fluorescence kinetic assays were performed in an SLM 8000 spectrofluorimeter (SLM Instruments, Inc., Urbana, IL) with stirred cell suspensions in a temperature-regulated cuvette holder. Solutions of 1-palmitoyl-2-oleoyl-phosphatidylcholine vesicles containing benzo(a)pyrene plus a fluorescence quencher, *N*-2,4-dinitrophenyl-*N*,*N*-dioctadecylamine (16) were added to suspensions of fibroblasts or P388D$_1$ cells. Benzo(a)pyrene fluorescence intensity was recorded as a function of time using excitation and emission wavelengths of 365 nm and 407 nm, respectively.

Analysis of kinetic data was performed by nonlinear least squares regression with respect to a monoexponential function. Data points were manually entered into an Apple II Plus microcomputer (Apple Computer, Inc., Cupertino, CA). The analytical program involved a reiteritive procedure and stringent criteria for convergence. Results of the analysis were evaluated by comparative plots of fitted curves and measured data points, standard deviation of data points from the fitted line, standard deviations for rate constant, and initial and final values, and analysis of correlation of error in these parameters.

RESULTS

Normal human fibroblasts metabolized benzo(a)pyrene very slowly, if at all, as illustrated in Fig. 1 and Table I. Thus, the interpretation of increase in cellular fluorescence, as an accurate index of cellular uptake of benzo(a)pyrene, is not complicated by the formation of metabolic products. Benzo(a)pyrene metabolism was studied in parallel with C3H/10T ½ mouse fibroblasts, which have been shown to have significant benzo(a)pyrene metabolic capacity (35). C3H/10T ½ cells produced fourfold more metabolites per milligram of cell protein in 24 h than did normal human fibroblasts. Less than 5% of the radioactivity was present as metabolites in

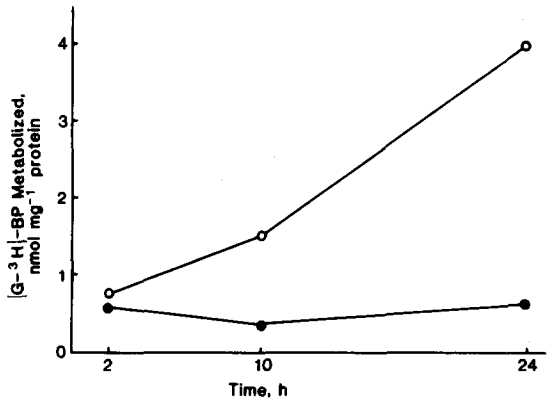

FIGURE 1 Benzo(a)pyrene metabolism in cultured cells. Normal human fibroblasts (●) and C3H/10T ½ murine fibroblasts (○) were incubated at 37°C in the presence of 50 $\mu g/ml^{-1}$ LDL containing [G-^{3}H]benzo(a)pyrene. A total of 10 nmol benzo(a)pyrene was added to each plate. For each cell type, duplicate dishes were incubated for 2 h at 4°C. Approximately 2% of total counts were identified as metabolites in these control plates. Data are expressed as total nanomoles of metabolites recovered from cells and media, corrected for the values at 4°C, and normalized per milligram of cell protein.

TABLE I

Comparative Metabolism of Benzo(a)pyrene in Normal Human Fibroblasts and Murine C3H/10T ½ Fibroblasts

Cell type	Incubation time*		Cells	Media	BP in metabolites
	4°C	37°C	nmol BP metabolites mg^{-1} protein		% of original radioactivity
Normal human fibroblast	2		0.11	0.58	2.5
		2	0.14	1.14	4.3
		10	0.14	0.91	3.8
		24	0.25	1.06	4.8
C3H/10T ½	2		0.14	0.68	2.3
		2	0.19	1.40	4.3
		10	0.33	1.99	5.6
		24	0.52	4.27	12.5

BP, benzo(a)pyrene.
* Time in hours.

fibroblast dishes, in contrast to 12% of total benzo(a)pyrene in C3H/10T ½ dishes in 24 h. P388D$_1$ cells were also examined for metabolic activity in a similar fashion, with negative results (data not shown).

Benzo(a)pyrene was presented to cells as a noncovalent component of LDL. Benzo(a)pyrene was solubilized in the hydrophobic core of lipoproteins, as demonstrated by its fluorescence spectrum in LDL (Fig. 2). When the same amount of benzo(a)pyrene in ethanolic solution was injected into aqueous buffer, the spectrum revealed that most of the benzo(a)pyrene was present as microcrystalline aggregates.

The cellular benzo(a)pyrene mass was obtained by quantification of [G-^{3}H]benzo(a)pyrene uptake. Fig. 3 shows the result of cell filtration assays in which 1×10^6 cells in stirred suspensions were exposed to increasing concentrations of LDL labeled with [G-^{3}H]benzo(a)pyrene. At the highest level of benzo(a)pyrene-LDL used, 5 mg of LDL protein·ml^{-1} and 1 mM benzo(a)pyrene, cellular accumulation of benzo(a)pyrene from LDL was $\sim 1.5 \times 10^{-15}$ mol benzo(a)pyrene per cell. With an estimated cell volume based on dimensions of $40 \times 30 \times 10$ μm, this corresponds to an average cellular concentration of ~150 μM. Benzo(a)pyrene was not uniformly distributed throughout any cell, however, and as will be described, often distinctly accumulated in regions comprising only a fraction of the total cell volume.

The time-dependent increase in the cellular fluorescence of benzo(a)pyrene is plotted in Fig. 4 for a typical experiment in which cells were exposed to 50 mg·ml^{-1} benzo(a)pyrene-LDL. Mean intensity values and intensities corresponding to the brightest intracellular areas were within the limits of detection and the linear response range of the video camera as determined by the fluorescence intensities of ethanolic solutions containing 0.1–200 μM benzo(a)pyrene.

The uptake of benzo(a)pyrene from lipoproteins into cells was independent of endocytosis of the lipoprotein carrier, even in cells that expressed receptors for LDL. Evidence for this was shown by the different rates of uptake of benzo(a)pyrene and dil when both probes were incorporated into the same lipoprotein. Because of the differences in spectral properties of the two probes, their cellular fluorescence was quantified independently. Cellular uptake of benzo(a)pyrene oc-

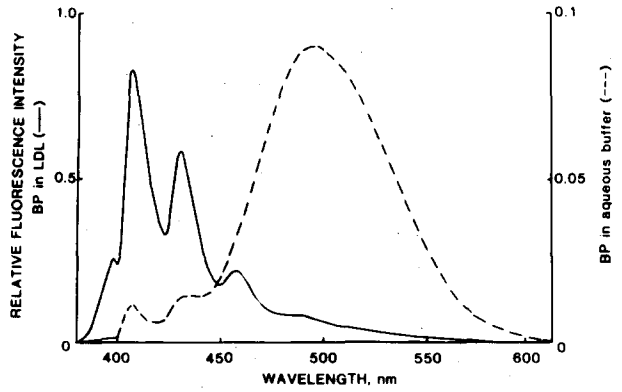

FIGURE 2 Spectral characteristics of benzo(a)pyrene solubilized in LDL and dispersed as microcrystals. Spectrum *A* (——): 10 μM benzo(a)pyrene as a component of LDL. Spectrum *B* (- - -): 10 μM benzo(a)pyrene prepared by injection of a 1-mM ethanolic solution of benzo(a)pyrene into aqueous buffer. The intensity scale for *A* is 10-fold greater than for *B*.

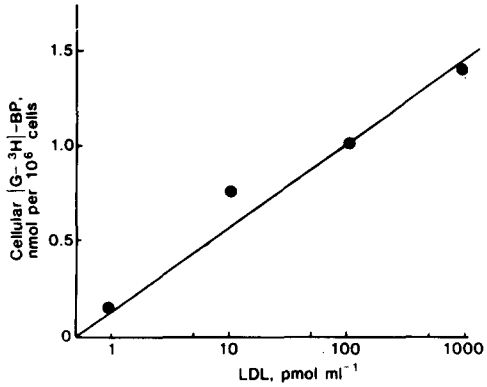

FIGURE 3 Cellular uptake of [G-^{3}H]benzo(a)pyrene. Increasing amounts of [G-^{3}H]benzo(a)pyrene-LDL were added to 2 ml of stirred suspensions of 2×10^6 P388D$_1$ macrophages. 50-μl aliquots were taken after 20 min to separate cells and incubation solution by filtration through glass fiber filters. Background values of 1–5% of total counts were obtained for solutions without cells, and these values were subtracted from filter counts. Specific activity of benzo(a)pyrene was 130 cpm·$pmol^{-1}$, with ~400 pmol of benzo(a)pyrene per picomole of LDL.

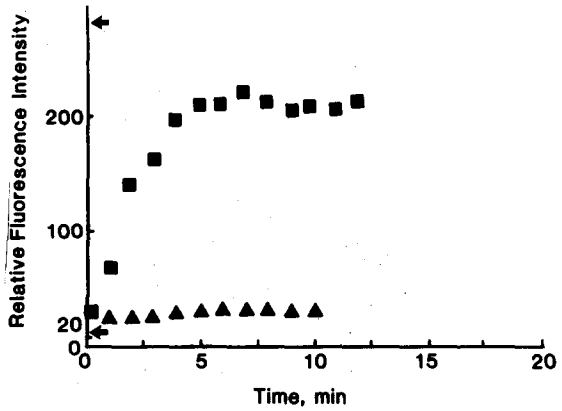

FIGURE 4 Cellular accumulation of benzo(a)pyrene. Medium containing 50 $\mu g \cdot ml^{-1}$ benzo(a)pyrene-labeled LDL was added to viable human fibroblasts on the microscope stage. Fluorescence intensity in a single field was sampled at the indicated times. Temperature was maintained at approximately 37°C. Neutral-density filters attenuated excitation light to 1% of maximum. Mean intensities over the field (▲), and upper range values for the field (■) are plotted as a function of time. Arrows at the abscissa designate limits of detection and range of linearity as determined by calibration with ethanolic solutions of benzo(a)pyrene, which were 0.1 and 200 μM, respectively.

curred within minutes and remained unchanged after ~10 min (Fig. 5), while cellular accumulation of the dil-labeled LDL required hours (Figs. 6 and 7). DiI has been shown to remain with LDL during the course of LDL endocytosis (29). Furthermore, when fibroblasts, which do not have specific receptors for HDL (11), were exposed to HDL labeled with both dil and benzo(a)pyrene, the time course of benzo(a)pyrene uptake was the same as that observed with LDL, while essentially no dil fluorescence was detected (Fig. 8). Fibroblasts, preincubated with lipoprotein-deficient medium to induce LDL receptors, did not take up benzo(a)pyrene faster or to a greater extent than noninduced cells. Cells fixed with 2% formaldehyde also accumulated benzo(a)pyrene from lipoproteins with the same rate and extent to produce the same pattern of intracellular localization as did viable cells examined in parallel. Cellular uptake and distribution of benzo(a)pyrene is therefore a spontaneous physical event that does not require metabolic processes, and the rate is not influenced by the presence or absence of receptors for the lipoprotein carrier.

The rate of cellular uptake of benzo(a)pyrene has been determined by three different techniques. Table II summarizes the rate constants for incorporation of benzo(a)pyrene by living and fixed cells as a function of temperature, lipophilic donor, and method of analysis. With digital fluorescence-imaging microscopy, the fluorescence intensity of each pixel in the image was measured. Fig. 9 shows the time-dependent increase in mean cellular fluorescence. The data were analyzed by nonlinear least squares regression with respect to a monoexponential function. The rate constants for cellular accumulation was 0.39 min^{-1} at 37°C and 0.25 min^{-1} at 23°C.

To confirm the rate constants measured by fluorescence microscopy, cell suspensions were mixed with 1-palmitoyl-2-oleoyl-phosphatidylcholine vesicles containing benzo(a)-pyrene and a nonexchangeable quencher, *N*-2,4-dinitrophenyl-*N*,*N*-dioctadecylamine. Increase in fluorescence intensity as a function of time was followed in a fluorimeter as benzo(a)pyrene transferred from quenched vesicles to cells. The rate constant for cellular uptake of benzo(a)pyrene was 0.21 min^{-1} at 21°C. Stirred cell suspensions were also mixed with LDL containing [G-^{3}H]benzo(a)pyrene. Aliquots taken at selected time intervals were rapidly filtered through glass fiber filters to trap cells and associated benzo(a)pyrene. The rate constants determined with this method was about 0.29 min^{-1} at 25°C. Experiments with cells in suspension performed with either fibroblasts or P388D$_1$ macrophages gave identical results. Thus, regardless of method or cell type used, uptake of benzo(a)pyrene into cells at room temperature occurs with a halftime of ~2 min. Only digital fluorescence-imaging microscopy, however, demonstrated the topographic heterogeneity of the intracellular location of benzo(a)pyrene.

The sampling area of this imaging microscopy system at the object plane was ~0.0625 μm^2 per pixel. Analysis of the increase in fluorescence intensity with time was performed on single pixels or small numbers of pixels corresponding to discrete intracellular locations and organelles. This analysis of the increase in benzo(a)pyrene fluorescence at discrete subcellular locations in individual cells did not identify any significant differences in rate constants for benzo(a)pyrene accumulation. However, due to a combination of the limited modulation transfer function of the camera (36) and optical diffusion of fluorescence in a light-scattering medium (i.e., cytoplasm), this question cannot be resolved without the application of computer-based mathematical deblurring procedures (36).

The amount of benzo(a)pyrene in different cellular locations varied greatly as determined by fluorescence intensity (Figs. 5, 7, and 8). For reference, the relative fluorescence intensities of 10 μM benzo(a)pyrene at the emission maximum of 405 nm were 1.0, 1.1, 1.3, and 2.0 in acetonitrile, ethanol, cyclohexane, and 1-palmitoyl-2-oleoyl-phosphatidylcholine vesicles, respectively. Because benzo(a)pyrene fluorescence was a linear function of concentration, and the relative fluorescence intensity of benzo(a)pyrene in different hydrophobic environments was similar, these results indicated that benzo(a)pyrene partitioned selectively into discrete subcellular locations.

LDL labeled with both benzo(a)pyrene and dil delivered both probes to cells simultaneously, but spatial analysis showed that the intracellular locations of the two fluorophores were distinctly different. The left panel of Fig. 10 (top left image) shows a fibroblast labeled with both dil and benzo(a)pyrene. The corresponding phase images are shown in the right panel of Fig. 10. The fluorescence images were viewed simultaneously by storing each image in a separate memory plane. Superimposition of the benzo(a)pyrene fluorescence image on the dil fluorescence image demonstrated unequivocally the distinct locations of the two fluorophores.

Identification of which cellular structures accumulate benzo(a)pyrene was achieved with a series of experiments using different organelle-specific fluorescent probes. Endocytosis of LDL delivers dil to lysosomes (10). Because dil is positively charged at low pH, it accumulates in these acidic compartments. To confirm the localization of dil, fibroblasts were grown in lipoprotein-deficient medium and then incubated with dil-labeled LDL for 2–4 h. Live cells were then exposed to 5 $\mu g \cdot ml^{-1}$ acridine orange to identify acidic compartments (37). The left center image of Fig. 8 (left) shows the coincidence of DiI and acridine orange fluorescence, indicating co-localization in acidic intracellular compartments. Benzo(a)pyrene fluorescence was not associated with

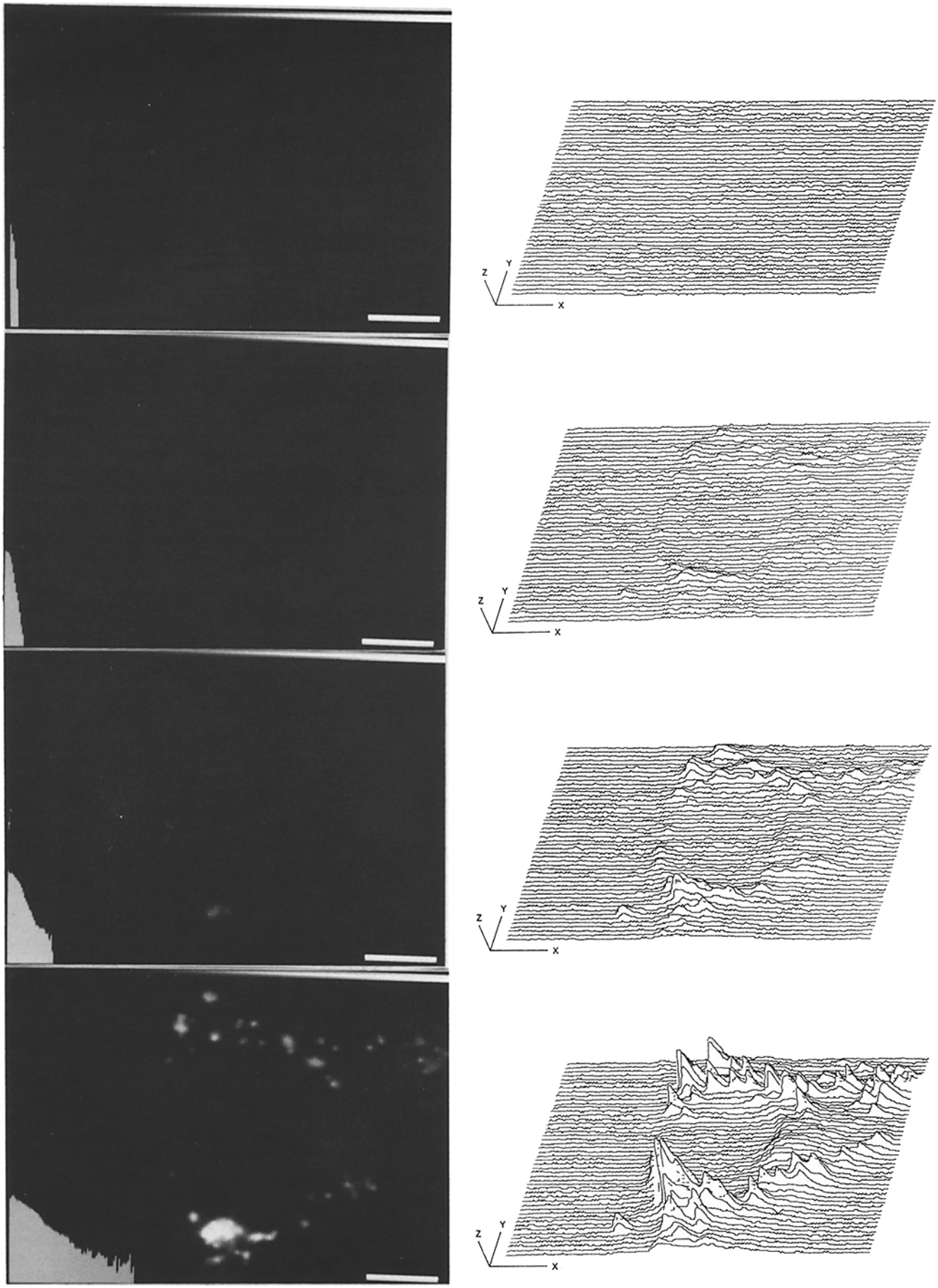

FIGURE 5 Cellular accumulation of benzo(a)pyrene by viable cells. 50 $\mu g \cdot ml^{-1}$ LDL containing either dil or benzo(a)pyrene was added in medium to cells on the microscope stage at 37°C. At the times indicated, cells were exposed for 1 s to excitation light attenuated to 1% for benzo(a)pyrene and 60% for dil. Cells had been preincubated for 2 d in lipoprotein-deficient medium to induce the expression of LDL receptors. (*Left images*) Benzo(a)pyrene fluorescence at 0.017, 1, 2, and 4 min, respectively. (*Right*) The isometric projections (22) illustrate the pixel-by-pixel time-dependent increases in intensity values for benzo(a)pyrene fluorescence. The corresponding digital images are immediately to the left of each projection.

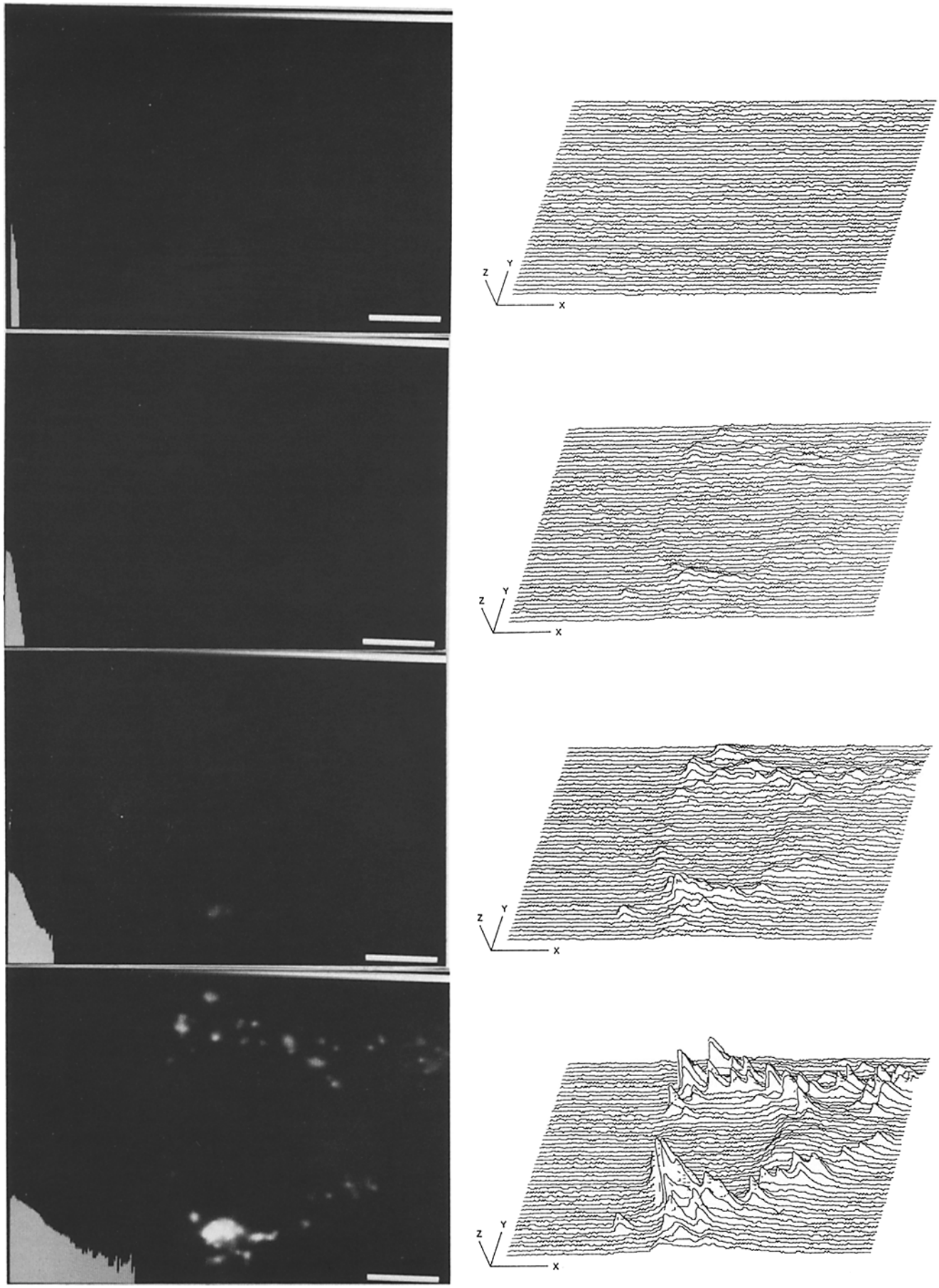

FIGURE 6 Cellular accumulation of LDL by viable cells. The experimental conditions are described in the legend to Fig. 5, except the excitation light was attentuated 60% to observe dil without photobleaching. (*Left images*) Dil-LDL fluorescence at 5, 15, 30, and 60 min, respectively. (*Right*) The isometric projections (22) illustrate the pixel-by-pixel time-dependent increases in intensity values for dil fluorescence. The corresponding digital images are immediately to the left of each projection.

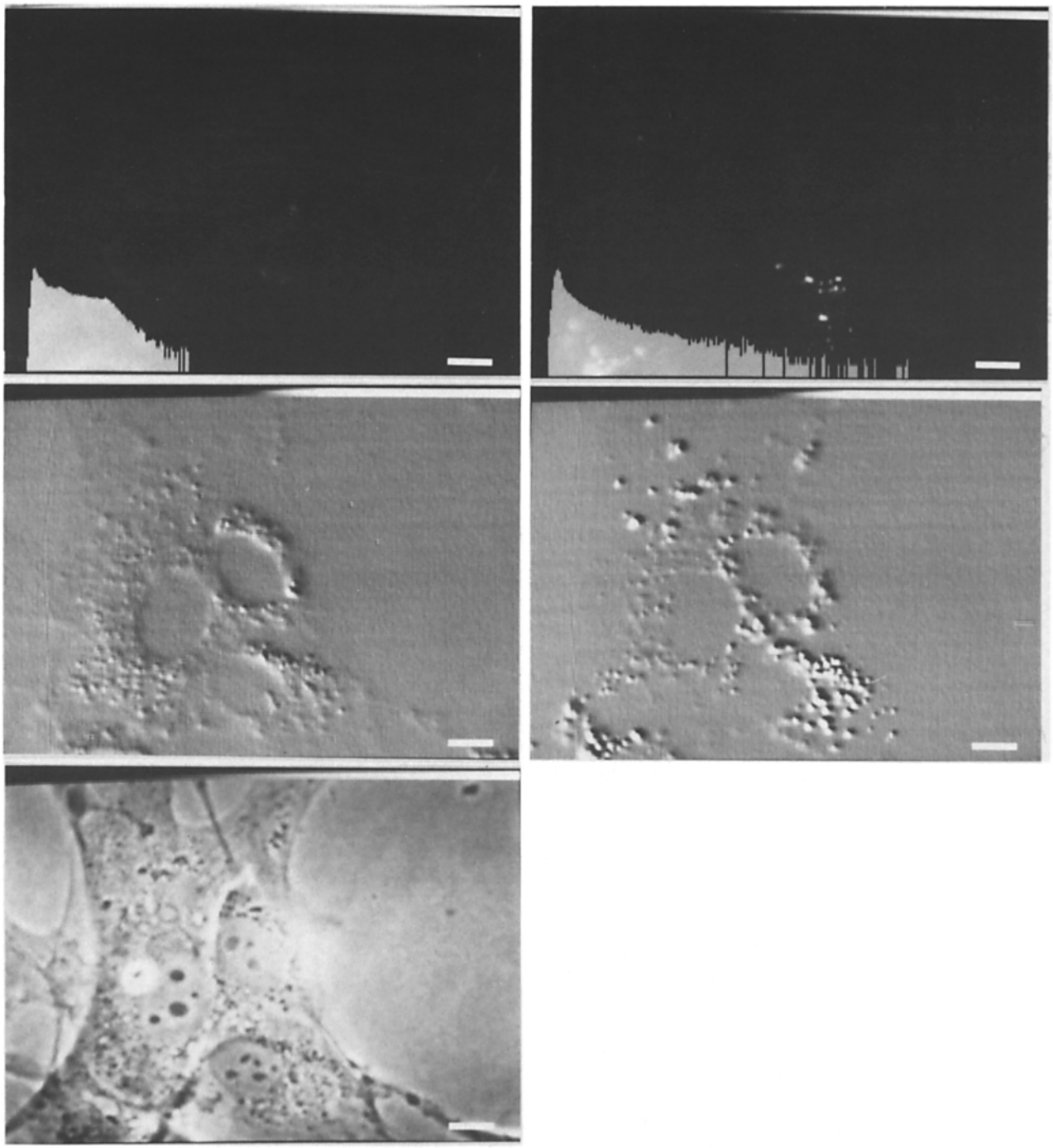

FIGURES 7 and 8 Comparison of benzo(a)pyrene uptake from HDL and LDL. Normal human fibroblasts on glass coverslips were preincubated in lipid-deficient medium for 2 d, and then incubated for 4 h at 37°C with medium containing either LDL or HDL. The lipoproteins were labeled with both dil and benzo(a)pyrene. Final benzo(a)pyrene concentration was 2.1 μM. Dil labeling was ~6 molecules per HDL and ~18 per LDL. LDL concentration was 30 $\mu g \cdot ml^{-1}$ and HDL concentration was 182 $\mu g \cdot ml^{-1}$. Cells were washed three times with 0.04 M Tris (pH 7.4) containing 5 $mg \cdot ml^{-1}$ bovine serum albumin, fixed, and placed in a Bionique chamber for viewing. Excitation light was attenuated to 5% for benzo(a)pyrene uptake and to 40% for dil-LDL uptake. The derivative images were obtained by subtraction of the appropriate shifted images from the original images and displaying the differences. The shifted images were created by incrementing the x,y coordinates of each pixel by 3 to the right and 3 to the top. Fig. 7 (*left images*) (*top to bottom*) Benzo(a)pyrene fluorescence, the derivative image of benzo(a)pyrene fluorescence, and the phase image of the cells, respectively. (*Right images*) (*top and bottom*) dil fluorescence of LDL, and the derivative image of dil fluorescence, respectively. Fig. 8 (*Left images*) (*top to bottom*) Benzo(a)pyrene fluorescence, the derivative image of benzo(a)pyrene fluorescence, and the phase image of the cells, respectively. (*Right images*) (*top and bottom*) dil fluorescence of HDL, and the derivative image of dil fluorescence, respectively.

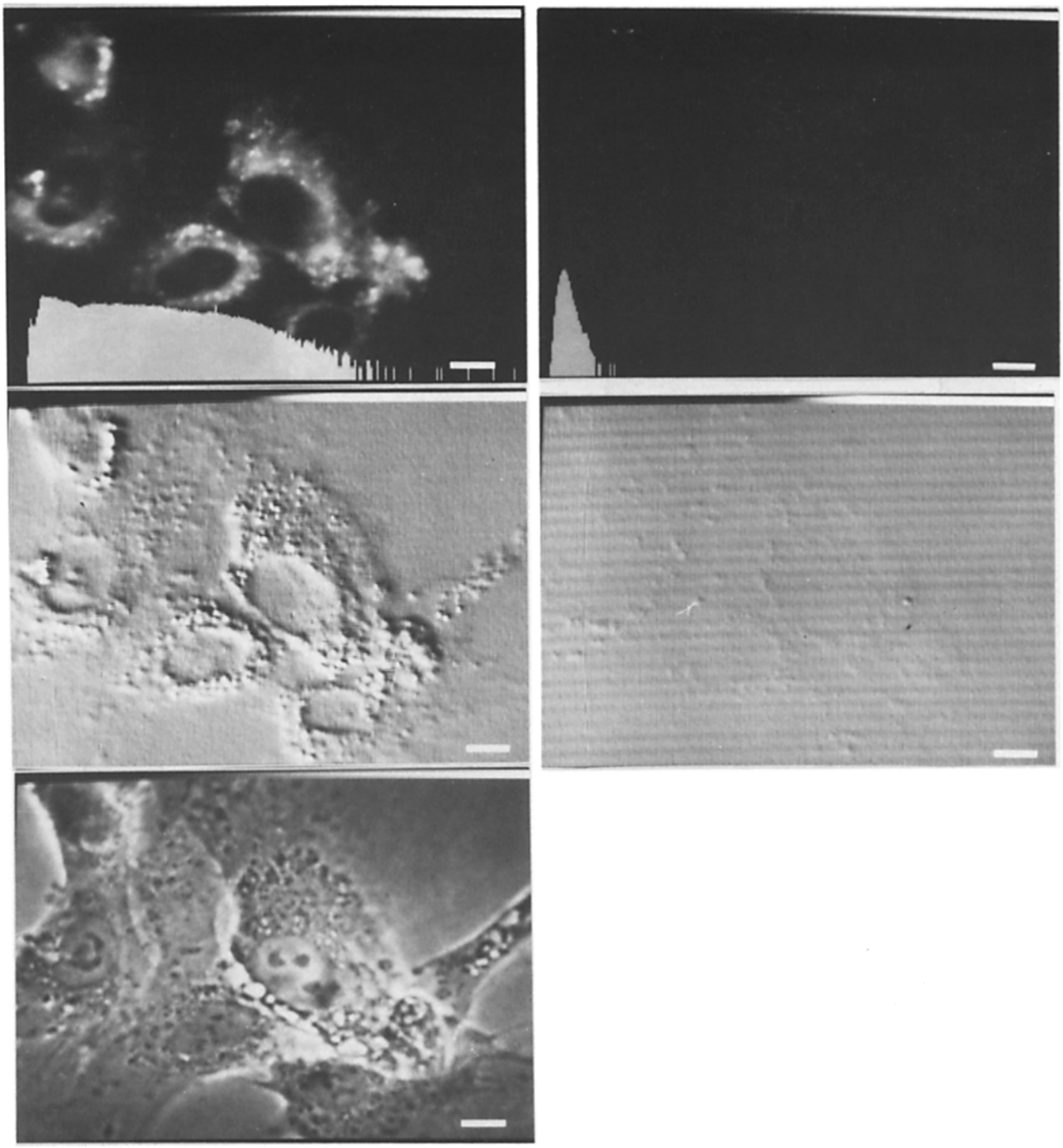

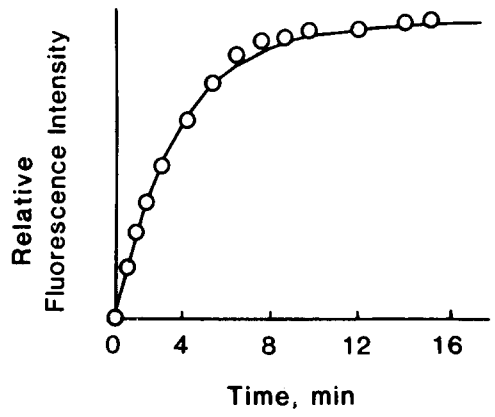

acridine orange fluorescence (Fig. 10, left bottom image).

The location of benzo(a)pyrene fluorescence was also compared with that of two other vital fluorescence probes, rhodamine-123 which is specific for mitochondria (38), and a cholesterol analog, NBD-cholesterol (27). From inspection of the images in the left panel of Fig. 10, it is apparent that

FIGURE 9 Kinetics of benzo(a)pyrene uptake by viable fibroblasts. At time zero, medium containing 50 $\mu g \cdot ml^{-1}$ benzo(a)pyrene-labeled LDL was added to fibroblasts at 37°C on the microscope stage. Open circles represent mean fluorescence intensities for the field containing 1–3 cells at the indicated times. The solid line represents analysis of the data with respect to a monoexponential function. The rate constant for uptake was 0.39 min^{-1}.

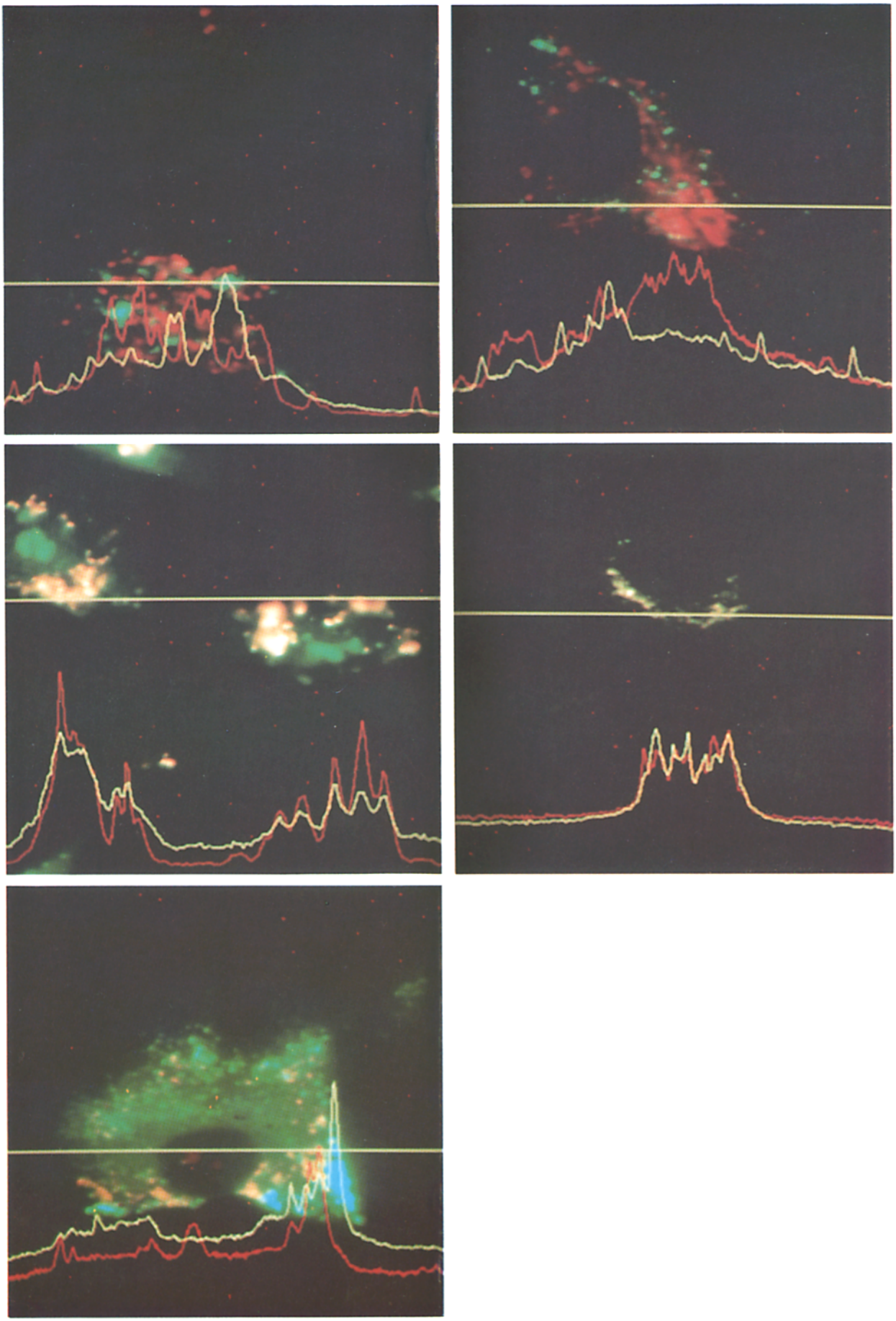

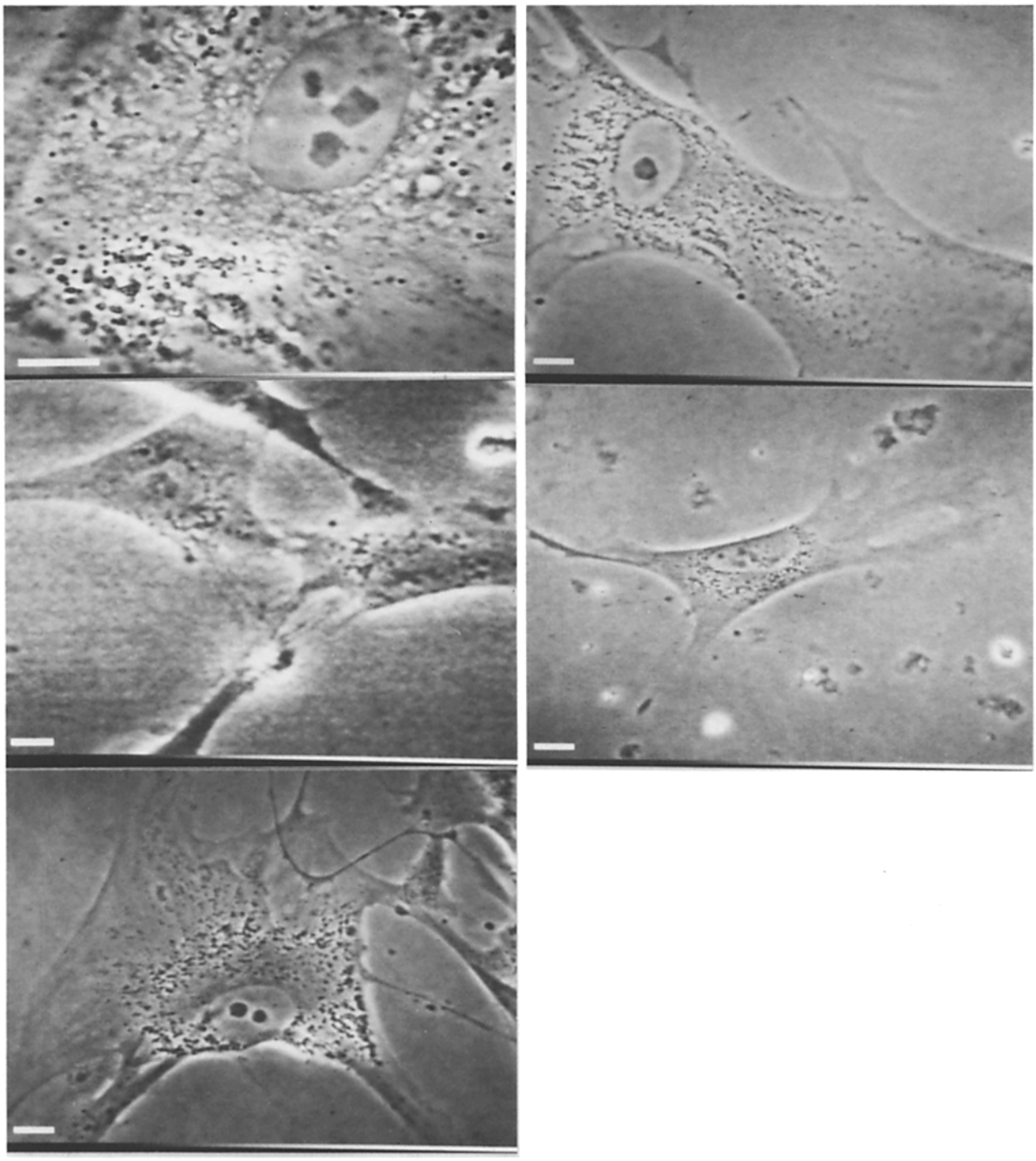

FIGURE 10 Comparison of spatial distribution of benzo(a)pyrene fluorescence in fibroblasts with fluorescence of DiI, acridine orange, rhodamine-123, and NBD-cholesterol. Fibroblasts induced for LDL receptors were incubated for 6 h at 37°C in the presence of 50 $\mu g \cdot ml^{-1}$ LDL containing both benzo(a)pyrene and dil. Cells were washed 2 times with 0.15 M NaCl and fixed with 2% formaldehyde before viewing. Labeling procedures used with the other fluorescent probes are described in Materials and Methods. To compare the distribution of two fluorescent probes, the phase images for the respective fluorescent images were superimposed by computer alignment of two memory planes. This procedure was necessary to correct misalignment originating from the nonparfocal nature of the filter cubes. Either a red or blue-green color was assigned to the two image channels for display of the fluorescence images identified below. With this combination of pseudocolors, regions of overlapping intensity in each image appear in white. The horizontal cursor identifies the pixel rows, the fluorescence intensity values of which are displayed as either a red or white intensity profile at the bottom of each panel. (*Left page*) (*left top images*) DiI (red color and red intensity profile), benzo(a)pyrene (blue-green color and white intensity profile). (*Left center images*) DiI (red color and red intensity profile), acridine orange (blue-green color and white intensity profile). (*Left bottom images*) Acridine orange (red color and red intensity profile), benzo(a)pyrene (blue-green color and white intensity profile). (*Right top images*) Rhodamine-123 (red color and red intensity profile), benzo(a)pyrene (blue-green color and white intensity profile). (*Right bottom images*) NBD--cholesterol (red color and red intensity profile), benzo(a)pyrene (blue-green color and white intensity profile). (Right page). The phase images correspond to their respective superimposed fluorescence images on the facing page. Bar, 10 μm.

TABLE II

Rate Constants for Uptake and Efflux of Benzo(a)pyrene by Human Fibroblasts

	Temperature	k	Cell condition	Method*
	°C	min^{-1}		
Donors				
LDL	37	0.39 (±0.04)	live	a
	22	0.29 (±0.03)	fixed	a
	23	0.25 (±0.08)	live	b
HDL	37	0.34 (±0.08)	live	a
	21	0.32 (±0.04)	fixed	a
	26	0.29 (±0.03)	live	b
VLDL	26	0.33 (±0.04)	live	b
POPC vesicles	21	0.21 (±0.03)	live	c
Acceptors				
HDL	22	0.26 (±0.04)	fixed	a
POPC	37	0.34 (±0.03)	live	c

The values in parentheses are standard deviations of data points from their fitted curves. The vesicles were 1-palmitoyl-2-oleylphosphatidylcholine (POPC).

* a, fluorescence microscopy; b, spectrofluorimetry; c, [G-^{3}H]benzo(a)pyrene filter assay.

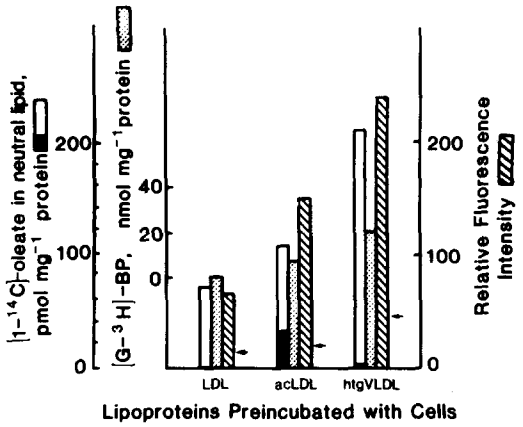

FIGURE 11 Relationship of cellular neutral lipid content, [G-^{3}H]-benzo(a)pyrene uptake, and benzo(a)pyrene fluorescence. Mouse peritoneal macrophages were incubated for 38 h with 50 $\mu g \cdot ml^{-1}$ LDL, acLDL, or htg VLDL, in addition to [1-^{14}C]oleate complexed with bovine serum albumin. Cells were then incubated for 1 h with [G-^{3}H]benzo(a)pyrene-LDL. Quantification of [1-^{14}C]-oleate and [G-^{3}H]-benzo(a)pyrene in cells grown in parallel is described in Materials and Methods. The fluorescence intensity of cells on coverslips was digitized with a gray scale of 0–255. Height of the striped bar represents upper range intensity values for each image, and arrows designate mean intensity values for the entire field. The open and closed bars represent the amount of triglyceride and cholesteryl ester, respectively, in the neutral lipid fraction of the cell extract.

TABLE III

Effect of Intracellular Lipid on Benzo(a)pyrene Accumulation

Lipoprotein in preincubation medium	Triglyceride	Cholesteryl ester	Benzo(a)pyrene	Fluorescence intensity	
				Mean	Upper range
	pmol [1-^{14}C]oleate mg^{-1} protein		*nmol mg^{-1} protein*		
LDL	67	0.8	10	13	66
acLDL	85	66	12	18	150
htg VLDL	210	3	15	46	240

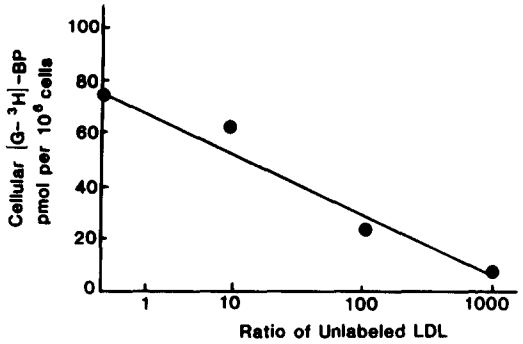

FIGURE 12 Equilibrium distribution of benzo(a)pyrene between cells and LDL as a function of extracellular LDL concentration. LDL (0.5 μg) containing 100 pmol [G-^{3}H]benzo(a)pyrene was added to 1 ml of a stirred cell suspension containing 10^6 cells and indicated amounts of unlabeled LDL. After 20 min at room temperature, aliquots were removed and filtered. Cells retained on glass fiber filters were counted to quantify cellular uptake of benzo(a)pyrene.

rhodamine-123 and benzo(a)pyrene did not distribute in the same intracellular location (top right), but that NBD-cholesterol and benzo(a)pyrene were distinctly co-localized (bottom right).

The co-localization of benzo(a)pyrene and the fluorescent cholesterol analog suggests that benzo(a)pyrene partitions selectively into cytoplasmic lipid droplets. Partitioning of benzo(a)pyrene into intracellular lipid droplets is not unexpected, in view of its lipophilic nature. Moreover, benzo(a)-pyrene has been used previously as a cytochemical stain for lipid (39). Because of the partitioning of benzo(a)pyrene, intracellular accumulation of lipid should produce increased benzo(a)pyrene accumulation. To demonstrate this relationship, mouse peritoneal macrophages were incubated with acLDL (34) or htg VLDL (25), lipoproteins that produce large intracellular accumulations of cholesteryl ester or triglyceride in these cells, respectively. Cells incubated with acLDL incorporated ~6.6 pmol and 8.5 pmol·mg^{-1} protein of [1-^{14}C] oleate into cholesteryl esters and triglycerides, respectively. Cells incubated with htg VLDL incorporated 3.0 pmol and 210 pmol·mg^{-1} protein [1-^{14}C]oleate into cholesteryl esters and triglycerides, respectively. The amount of benzo(a)pyrene incorporated by these cells increased with increased lipid accumulated, measured by [G-^{3}H]benzo(a)pyrene and by cellular fluorescence intensity (Fig. 11; Table III). After preincubation with acLDL, 24 nmol benzo(a)pyrene was accumulated per nanomole [1-^{14}C]oleate esterified. After preincubation with htg VLDL, cells accumulated 34 nmol benzo(a)pyrene per nanomole [1-^{14}C]oleate esterified.

When LDL labeled with [G-^{3}H]benzo(a)pyrene was added to cell suspensions containing increasing concentrations of unlabeled LDL, the rate constants for benzo(a)pyrene uptake were unchanged. However, the net amount of cellular benzo(a)pyrene decreased as a function of increasing amount of unlabeled LDL added to the extracellular solution (Fig. 12). Thus, the equilibrium distribution of benzo(a)pyrene into cells was controlled by the relative lipid volume of cells and extracellular particles.

DISCUSSION

Mechanism of Cellular Uptake

The importance of partitioning and solubility characteristics of carcinogenic compounds on their distribution and metabolism has been largely ignored. Consideration of the

physical properties of polycyclic aromatic hydrocarbons suggests that it is reasonable to expect benzo(a)pyrene metabolism would be influenced by its lipid solubility and partitioning into membranes and lipid droplets. It has been noted (40–42) that the apparent K_m measured for cytochrome P_{450} substrates is dependent on concentrations of membranes or cells. Recently, Backes et al. (43) addressed the mechanism of this phenomenon by calculating microsomal partition coefficients for a series of aromatic substrates of increasing molecular size. Nemoto and Takayama (44) found that the addition of serum to microsome suspensions resulted in large increases in benzo(a)pyrene metabolism, at least in part due to increased solubilization of benzo(a)pyrene.

In most metabolic studies, either in purified reconstituted P_{450} systems or in cell culture, benzo(a)pyrene is usually added as a concentrated solution in organic solvent (45, 46). The observation of crystalline benzo(a)pyrene in lysosomes of fibroblasts, which involved the addition of benzo(a)pyrene at high concentrations in dimethylsulfoxide to the culture medium, most likely involved phagocytosis of particulate hydrocarbon. Spectral analysis of benzo(a)pyrene (3, 4) demonstrates that benzo(a)pyrene is dispersed as microcrystals by this method. Lakowicz et al. (5) have shown significantly slower rates of solubilization of benzo(a)pyrene from microcrystals to membranes, compared with the rates for benzo(a)pyrene solubilized by adsorption to particulate material. Thus, any kinetic data for benzo(a)pyrene metabolism involving this mechanism of presentation is therefore difficult, if not impossible, to interpret. In this study we have avoided this experimental ambiguity by presenting cells with benzo(a)pyrene solubilized in the hydrophobic core of plasma lipoproteins.

It has been shown (6) that benzo(a)pyrene in plasma is associated with lipoproteins, and to the greatest extent with LDL in normolipemic plasma. By exposing both living and fixed cells to LDL containing benzo(a)pyrene, we have shown by digital fluorescence microscopy that the cellular uptake of benzo(a)pyrene occurs at the same rate and is therefore independent of LDL endocytosis. This conclusion supports the work of Remsen and Shireman (20), who compared benzo(a)pyrene uptake from LDL by both normal and receptor-negative fibroblasts, at single time points. Although these authors did not exclude low affinity receptor-independent pathways, they correctly concluded that a passive diffusion process was responsible for benzo(a)pyrene transfer to the plasma membrane. In the present study, digital fluorescence microscopy provides topographic information about the intracellular location of benzo(a)pyrene. Thus, mechanistically, passive transfer appears to be solely responsible for redistribution of benzo(a)pyrene from extracellular lipoproteins to the plasma membrane, and from the plasma membrane to intracellular compartments. The time course of uptake and the intracellular localization of benzo(a)pyrene are clearly independent of that of the lipoprotein particle as indicated by the nontransferable fluorescent lipoprotein probe, dil.

The results from this investigation are not consistent with the conclusions reached by Shu and Bymun (47). These authors reported that the amount of benzo(a)pyrene excreted in the bile of rats injected with benzo(a)pyrene noncovalently associated with lipoproteins was dependent on the lipoprotein donor with which benzo(a)pyrene was originally associated. However, equilibration of benzo(a)pyrene among plasma lipoprotein classes occurs on a millisecond time scale (13). In that this equilibration is two orders of magnitude faster than benzo(a)pyrene entry into cells, rate constants for cell uptake and release of benzo(a)pyrene should be independent of the identity of the original lipoprotein donor, which we observe.

Intracellular Location of Benzo(a)pyrene

Intracellular location of benzo(a)pyrene has been compared with that of various fluorescent probes with known intracellular locations. These experiments indicate that benzo(a)pyrene is not predominantly located in acidic compartments or mitochondria, but concentrates in cytoplasmic lipid droplets (48, 49), as expected from its solubility properties and intracellular coincidence with a cholesterol analog. It should be noted that benzo(a)pyrene fluorescence is conspicuously absent from the nucleus. It is not possible, at present, to distinguish between fluorescence quenching and the presence of benzo(a)pyrene concentrations that are below the limits of detection. It seems unlikely that quenching accounts for the absence of benzo(a)pyrene fluorescence. Studies involving removal and replacement of nucleic acids and treatment of tissue with ethanol or buffers did not produce measurable effect on fluorescence intensity (50, 51).

Other attempts to identify the intracellular location of benzo(a)pyrene have employed subcellular fractionation (52–57). This method gives questionable results because of the rapid rate of benzo(a)pyrene partitioning. Autoradiography of subcellular locations of polycyclic aromatic hydrocarbons carcinogens suggest that these compounds associate with cell nuclei (57–59). However, the comprehensive study by Shires (50) of the effects of various preparative procedures showed that benzo(a)pyrene fluorescence in the nucleus cannot be detected except when ethanol, citrate, or acetate is used. Moreover, nuclear fluorescence was detected by Stora (60) in tissue sections from rats treated with benzo(a)pyrene only after 43 d. No nuclear fluorescence was detected before that time. These latter experiments involved embedding fixed tissue sections in paraffin, and deparaffinizing before viewing. Inasmuch as the solvents used for these experiments would remove all noncovalently bound benzo(a)pyrene, the nuclear fluorescence observed by Stora was not that of benzo(a)pyrene, but more likely a covalently immobilized metabolite of benzo(a)pyrene. The predominant intracellular location for benzo(a)pyrene reported in our study is consistent with its partitioning characteristics.

Transfer of benzo(a)pyrene between lipoprotein particles is two to three orders of magnitude faster than uptake by cells. The fact that the rate constants for cell uptake are the same, regardless of carrier size, suggests that the slow step in the entry of benzo(a)pyrene into cells occurs after the initial desorption process. Identification of the slow step in the process of cell uptake of benzo(a)pyrene is still under investigation, but it appears that the plasma membrane is the site of the rate-limiting step in the accumulation of polycyclic aromatic hydrocarbons by cells.

Increasing the concentration of extracellular unlabeled LDL does not alter the rate constant for benzo(a)pyrene uptake, but does decrease the net amount of benzo(a)pyrene entering cells. By contrast, increasing the amount of lipid present in cells produces increased cellular benzo(a)pyrene accumulation. Moreover, it is apparent that benzo(a)pyrene uptake by cells is a spontaneous transfer process from a donor hydrophobic particle to cellular lipid compartments. Spontaneous aqueous phase transfer is controlled by partitioning of the transferring species between one hydrophobic compartment and another. The extent of transfer of benzo(a)pyrene

into cells is determined by the equilibrium distribution between the relative hydrophobic volumes inside and outside the cell. Increasing cellular lipid content in vivo could result in increased benzo(a)pyrene accumulation in tissues and indicates a possible relationship between tissue lipid deposits and carcinogenesis.

This work was supported by grants from the Gulf Oil Foundation and the Robert A. Welch Foundation Q-343, grants HL-15648, HL-23741, and CA-31513 from the U.S. Public Health Service and grant R80-8773 from the Environmental Protection Agency. Additional funding was provided by Baylor College of Medicine. The Environmental Protection Agency does not necessarily endorse any commercial products used in this study. The conclusions represent the reviews of the authors and do not necessarily represent the opinions, policies or recommendations of the Environmental Protection Agency. Dr. Plant was predoctoral fellow (HL-07282) and Dr. Benson is a postdoctoral fellow (CA-07090), both supported by the U.S. Public Health Service.

Received for publication 18 June 1984, and in revised form 13 December 1984.

REFERENCES

1. Gelboin, H. V. 1980. Benzo(a)pyrene metabolism, activation, and carcinogenesis: role and regulation of mixed-function oxidases and related enzymes. *Physiol. Rev.* 60:1107–1166.
2. Berenblum, I. 1982. Sequential aspects of chemical carcinogenesis: skin. *In* Cancer: A Comprehensive Treatise. F. F. Becker, editor. Plenum Press, New York. Second ed. 451–461.
3. Mackay, D., and W. Y. Shiu. 1977. Aqueous solubility of polynuclear aromatic hydrocarbons. *J. Chem. Eng. Data.* 22:399–402.
4. Weinberger, R., and L. J. C. Love. 1984. Luminescence properties of polycyclic aromatic hydrocarbons on colloidal or microcrystalline suspensions. *Spectrochim. Acta.* 40A:49–55.
5. Lakowicz, J. R., D. R. Bevan, and S. C. Riemer. 1980. Transport of a carcinogen, benzo(a)pyrene, from particulates to lipid bilayers. *Biochim. Biophys. Acta.* 629:243–258.
6. Shu, H. P., and A. V. Nichols. 1979. Benzo(a)pyrene uptake by human plasma lipoproteins in vitro. *Cancer Res.* 39:1224–1230.
7. Chen, T. C., W. A. Bradley, A. M. Gotto, Jr., and J. D. Morrisett. 1979. Binding of the chemical carcinogen, *p*-dimethylaminoazobenzene by human plasma or low density lipoproteins. *FEBS (Fed. Eur. Biochem. Soc.) Let.* 104:236–240.
8. Grubbs, C. J., and R. C. Moon. 1973. Transport of orally administered 9,10-dimethyl-1,2-benzanthracene in the Sprague-Dawley rat. *Cancer Res.* 33:1785–1789.
9. Smith, L. C., H. J. Pownall, and A. M. Gotto, Jr. 1978. The plasma lipoproteins: structure and metabolism. *Annu. Rev. Biochem.* 47:751–777.
10. Smith, L. C., J. B. Massey, J. T. Sparrow, A. M. Gotto, Jr., and H. J. Pownall. 1983. Structure and dynamics of human plasma lipoproteins. *In* Supramolecular Structure and Function. G. Pifat and J. N. Herak, editors. Plenum Press, New York. 205–243.
11. Brown, M. S., J. R. Faust, and J. L. Goldstein. 1975. Role of the low density lipoprotein receptor in regulating the content of free and esterified cholesterol in human fibroblasts. *J. Clin. Invest.* 55:783–793.
12. Smith, L. C., and M. C. Doody. 1981. Kinetics of benzo(a)pyrene transfer between human plasma lipoproteins. *In* Chemical Analysis and Biological Fate: Polynuclear Aromatic Hydrocarbons. M. Cooke and A. J. Dennis, editors. Battelle Press, Columbus, OH. 615–624.
13. Pownall, H. J., D. L. Hickson, and L. C. Smith. 1983. Transport of biological lipophiles: effect of lipophile structure. *J. Am. Chem. Soc.* 105:2440–2445.
14. Doody, M. C., H. J. Pownall, Y. J. Kao, and L. C. Smith. 1980. Mechanism and kinetics of transfer of a fluorescent fatty acid between single-walled phosphatidylcholine vesicles. *Biochemistry.* 19:108–116.
15. Massey, J. B., A. M. Gotto, Jr., and H. J. Pownall. 1982. Kinetics and mechanism of the spontaneous transfer of fluorescent phospholipids between apolipoprotein-phospholipid recombinants: effect of the polar headgroup. *J. Biol. Chem.* 257:544–548.
16. Plant, A. L., H. J. Pownall, and L. C. Smith. 1983. Transfer of polycyclic aromatic hydrocarbons between model membranes: relation to carcinogencity. *Chem. Biol. Interact.* 44:237–246.
17. Poznansky, M. J., and S. Czekanski. 1979. Cholesterol exchange as a function of cholesterol/phospholipid mole ratios. *Biochem. J.* 177:989–991.
18. Damen, J., J. Regts, and G. Scherphof. 1981. Transfer and exchange of phospholipid between small unilamellar liposomes and rat plasma high density lipoproteins. *Biochim. Biophys. Acta.* 665:538–545.
19. Charlton, S. C., and L. C. Smith. 1982. Kinetics of transfer of pyrene and *rac*-1-oleyl-2-[4-(3-pyrenyl)butanoyl]glycerol between human plasma lipoproteins. *Biochemistry.* 21:4023–4030.
20. Remsen, J. F., and R. B. Shireman. 1981. Effect of low-density lipoprotein on the incorporation of benzo(a)pyrene by cultured cells. *Cancer Res.* 41:3179–3185.
21. Benson, D. M., A. L. Plant, J. Bryan, A. M. Gotto, and L. C. Smith. 1983. Digital fluorescence microscopy: kinetics of uptake of benzo(a)pyrene and of low density lipoproteins by living cells. *J. Cell Biol.* 97(2, Pt. 2):427a. (Abstr.)
22. Benson, D. M., A. L. Plant, J. Bryan, A. M. Gotto, Jr., and L. C. Smith. 1985. Digital fluorescence imaging microscopy: spatial heterogeneity of photobleaching rate constants in individual cells. *J. Cell Biol.* 100:1309–1323.
23. Willingham, M. C., and I. Pastan. 1978. The visualization of fluorescent proteins in living cells by video intensification microscopy (VIM). *Cell.* 13:501–507.
24. Havel, R. J., H. A. Eder, and J. J. Bragdon. 1955. The distribution and chemical composition of ultracentrifugally separated lipoproteins in human serum. *J. Clin. Invest.* 34:1344–1353.
25. Gianturco, S. H., W. A. Bradley, A. M. Gotto, Jr., J. D. Morrisett, and D. L. Peavy. 1982. Hypertriglyceridemic very low density lipoproteins induce triglyceride synthesis and accumulation in mouse peritoneal macrophages. *J. Clin. Invest.* 70:168–178.
26. Basu, S. K., J. L. Goldstein, R. G. W. Anderson, and M. S. Brown. 1976. Degradation of cationized low density lipoprotein and regulation of cholesterol metabolism in homozygous familial hypercholesterolemia fibroblasts. *Proc. Natl. Acad. Sci. USA.* 73:3178–3182.
27. Craig, I. F., D. P. Via, W. W. Mantulin, H. J. Pownall, A. M. Gotto, Jr., and L. C. Smith. 1981. Low density lipoproteins reconstituted with steroids containing the nitrobenzoxadiazole fluorophore. *J. Lipid Res.* 22:687–697.
28. Friedel, R. A., and M. Orchim. 1951. U.V. Spectra of Aromatic Compounds. John Wiley and Sons, Inc., New York. 52 pp.
29. Pitas, R. E., T. L. Innerarity, J. N. Weinstein, and R. W. Mahley. 1981. Acetoacetylated lipoproteins used to distinguish fibroblasts from macrophages *in vitro* by fluorescence microscopy. *Arteriosclerosis.* 1:177–185.
30. Cantor, C. R., and P. R. Schimmel. 1980. Biophysical Chemistry II. Techniques for the Study of Biological Structure and Function. W. H. Freeman and Co., San Francisco. 439.
31. Sernetz, M., and A. Thaer. 1973. Microcapillary fluorometry and standardization for microscope fluorometry. *In* Fluorescence Techniques in Cell Biology. A. Thaer and M. Sernetz, editors. Springer-Verlag, Berlin. 41–53.
32. Lowry, O. H., N. J. Rosebrough, A. L. Farr, and R. J. Randall. 1951. Protein measurement with the Folin phenol reagent. *J. Biol. Chem.* 193:265–275.
33. Selkirk, J. K., R. G. Croy, J. P. Whitlock, and H. V. Gelboin. 1975. In vitro metabolism of benzo(a)pyrene by human liver microsomes and lymphocytes. *Cancer Res.* 35:3651–3655.
34. Brown, M. S., J. L. Goldstein, M. Krieger, Y. K. Ho, and R. G. W. Anderson. 1979. Reversible accumulation of cholesteryl esters in macrophages incubated with acetylated lipoproteins. *J. Cell Biol.* 82:597–613.
35. Gehly, E. B., and C. Heidelberger. 1982. Metabolic activation of benzo(a)pyrene by transformable and nontransformable C3H mouse fibroblasts in culture. *Cancer Res.* 42:2697–2704.
36. Castleman, K. R. 1979. Digital Image Processing. John Wiley and Sons, Inc., New York. 257–60.
37. Robbins, E., P. I. Marcus, and N. K. Ganatas. 1964. Dynamics of acridine orange-cell interaction. II. Dye-induced ultrastructural changes in multivesicular bodies (acridine orange particles). *J. Cell Biol.* 21:49–62.
38. Siemens, A., R. Walter, L.-H. Liaw, and M. W. Berns. 1982. Laser-stimulated fluorescence of submicrometer regions within single mitochondria of rhodamine-treated myocardial cells in culture. *Proc. Natl. Acad. Sci. USA.* 79:466–470.
39. Berg, N. O. 1951. A histological study of masked lipids; stainability, distribution and functional variations. *Acta. Pathol. Microbiol. Scand.* 40(Suppl.):192.
40. Miller, A. G., and J. P. Whitlock. 1982. Efficient metabolism of benzo(a)pyrene at nanomolar concentrations by intact murine hepatoma cells. *Cancer Res.* 42:4473–4478.
41. Ebel, R. E., D. M. O'Keefe, and J. A. Peterson. 1978. Substrate binding to hepatic microsomal cytochrome P_{450}: influence of the microsomal membrane. *J. Biol. Chem.* 253:3888–3897.
42. Lu, A. Y. H., D. M. Jerins, and W. Levin. 1977. Liver microsomal epoxide hydrase hydration of alkene and arene oxides by membrane-bound and purified enzymes. *J. Biol. Chem.* 252:3715–3723.
43. Backes, W. L., M. Hogaboom, and W. J. Canady. 1982. The true hydrophobicity of microsomal cytochrome P-450 in the rat. *J. Biol. Chem.* 257:4063–4070.
44. Nemoto, N., and S. Takayama. 1982. Modulation of microsome-mediated benzo(a)pyrene-metabolism by serum. *Carcinogenisis.* 3:359–362.
45. Kocan, R. M., E. Y. Chi, N. Eriksen, E. P. Benditt, and M. L. Landolt. 1983. Sequestration and release of polycyclic aromatic hydrocarbons by vertebrate cells in vitro. *Environ. Mutagen.* 5:643–656.
46. Salmon, J.-M., C. Thierry, B. Serrou, and P. Viallet. 1981. Slower step of the polycyclic aromatic hydrocarbons metabolism: kinetic data from microspectrofluorometric techniques. *Biomedicine (Paris).* 34:102–107.
47. Shu, H. P., and E. N. Bymun. 1983. Systemic excretion of benzo(a)pyrene in the control and microsomally induced rat: the influence of plasma lipoproteins and albumin as carrier molecules. *Cancer Res.* 39:485–490.
48. Kruth, H. S., J. Avigan, W. Gamble, and M. Vaughan. 1979. Effect of cell density on binding and uptake of low density lipoprotein by human fibroblasts. *J. Cell Biol.* 83:588–594.
49. Kruth, H. S., J. Blanchette-Mackie, J. Avigan, W. Gamble, and M. Vaughan. 1982. Subcellular localization and quantification of cholesterol in cultured human fibroblasts exposed to human low density lipoprotein. *J. Lipid Res.* 23:1128–1135.
50. Shires, T. K. 1969. A fluorescence microscopic study of methodologic effects on the intranuclear distribution of benzo(a)pyrene. *Cancer Res.* 29:1277–1287.
51. Shires, T. J. 1966. An evaluation of possible intracellular nucleic acid quenching of carcinogenic hydrocarbon fluorescence. *Am. J. Anat.* 119:499–520.
52. Calcutt, G. 1958. The distribution of polycyclic hydrocarbons within the cells of some mouse and rat tissues. *Br. J. Cancer.* 12:149–160.
53. Fiala, S., and A. E. Fiala. 1959. Intracellular localization of carcinogen and its relationship to the mechanism of carcinogenesis of rat liver. *Br. J. Cancer.* 13:236–250.
54. Wiest, W. G., and C. Heidelberger. 1953. Interaction of carcinogenic hydrocarbons with tissue constituents. I. Methods. *Cancer Res.* 13:246–249.
55. Woodhouse, D. L. 1954. Experiments on the interaction of polycyclic hydrocarbons with epidermal constituents. *Br. J. Cancer.* 8:346–352.
56. Ekelman, K. B., and G. E. Milo. 1978. Cellular uptake, transport, and macromolecular binding of benzo(a)pyrene and 7,12-dimethylbenz(a)anthracene by human cells in vitro. *Cancer Res.* 38:3026–3032.
57. Bresnick, E., R. A. Liebelt, and J. C. Madix. 1967. The distribution of radioactivity within the hepatic cell after administration of labeled 3-methylcholanthrene. *Cancer Res.* 27:462–468.
58. Diamond, L., V. Defendi, and P. Brookes. 1967. The interaction of 7,12-dimethylbenz(a)anthracene with cells sensitive and resistant to toxicity induced by this carcinogen. *Cancer Res.* 27:890–897.
59. DiPaola, J. A., and M. R. Banerjee. 1967. Autoradiographic demonstration of ^{3}H-methylcholanthrene labeling of nuclear components of syrian hamster cells in vitro. *Proc. Natl. Acad. Sci. USA.* 58:123–126.
60. Stora, C. 1980. Cellular localization of chemical carcinogens studies by fluorescence microscopy. *Oncology.* 37:20–22.